A new class of peroxisome proliferator-activated receptor γ (PPARγ) agonists that inhibit growth of breast cancer cells: 1,1-Bis(3′-indolyl)-1-(*p*-substituted phenyl)methanes

Chunhua Qin,[1] Derek Morrow,[1] Jessica Stewart,[1] Kyle Spencer,[1] Weston Porter,[2] Roger Smith, III,[3] Timothy Phillips,[2] Maen Abdelrahim,[1] Ismael Samudio,[4] and Stephen Safe[1,4]

Departments of [1]Veterinary Physiology and Pharmacology, [2]Veterinary Anatomy and Public Health, and [3]Veterinary Pathobiology, College of Veterinary Medicine, Texas A&M University, College Station, TX; and [4]Institute of Biosciences and Technology, Texas A&M University System, Health Science Center, Houston, TX

Abstract

1,1-Bis(3′-indolyl)-1-(*p*-trifluoromethylphenyl)methane (DIM-C-pPhCF$_3$) and several *p*-substituted phenyl analogues have been investigated as a new class of peroxisome proliferator-activated receptor γ (PPARγ) agonists. Structure-activity studies in PPARγ-dependent transactivation assays in MCF-7 breast cancer cells show that 5–20 μM concentrations of compounds containing *p*-trifluoromethyl, *t*-butyl, cyano, dimethylamino, and phenyl groups were active, whereas *p*-methyl, hydrogen, methoxy, hydroxyl, or halogen groups were inactive as PPARγ agonists. Induction of PPARγ-dependent transactivation by 15-deoxy-Δ12,14-prostaglandin J2 (PGJ2) and DIM-C-pPhCF$_3$ was inhibited in MCF-7 cells cotreated with the PPARγ-specific antagonist *N*-(4′-aminopyridyl)-2-chloro-5-nitrobenzamide. In mammalian two-hybrid assays, DIM-C-pPhCF$_3$ and PGJ2 (5–20 μM) induced interactions of PPARγ with steroid receptor coactivator (SRC) 1, SRC2 (TIFII), and thyroid hormone receptor-associated protein 220 but not with SRC3 (AIB1). In contrast, DIM-C-pPhCF$_3$, but not PGJ2, induced interactions of PPARγ with PPARγ coactivator-1. C-substituted diindolylmethanes inhibit carcinogen-induced rat mammary tumor growth, induce differentiation in 3T3-L1 preadipocytes, inhibit MCF-7 cell growth and G$_0$/G$_1$-S phase progression, induce apoptosis, and down-regulate cyclin D1 protein and estrogen receptor α in breast cancer cells. These compounds are a novel class of synthetic PPARγ agonists that induce responses in MCF-7 cells similar to those observed for PGJ2. [Mol Cancer Ther. 2004;3(3):247–259]

Received 7/29/03; revised 1/5/04; accepted 1/9/04.

Grant support: NIH (ES09106) and the Texas Agricultural Experiment Station.

The costs of publication of this article were defrayed in part by the payment of page charges. This article must therefore be hereby marked advertisement in accordance with 18 U.S.C. Section 1734 solely to indicate this fact.

Requests for Reprints: Stephen Safe, Department of Veterinary Physiology and Pharmacology, College of Veterinary Medicine, Texas A&M University, 4466 TAMU, Veterinary Research Building 409, College Station, TX 77843-4466. Phone: (979) 845-5988; Fax: (979) 862-4929. E-mail: ssafe@cvm.tamu.edu

Introduction

Peroxisome proliferator-activated receptor γ (PPARγ) is a ligand-activated transcription factor and a member of the nuclear hormone receptor (NHR) superfamily (1–7). PPARγ is highly expressed in fatty tissues and up-regulated in tumors. PPARγ participates in several metabolic pathways including adipocyte differentiation, insulin resistance, atherosclerosis, and hypertension, and this receptor is a major target for development of new drugs to treat metabolic diseases (1–7). PPARγ, like other members of the NHR superfamily, contains a modular structure that includes a NH_2-terminal activation function 1 and a COOH-terminal activation function 2, which also binds ligands. The DNA binding domain of PPARγ and other NHRs contain two zinc fingers, and PPARγ partners with the retinoid X receptor (RXR) to bind PPAR response elements (PPRE) containing AGGNCA half-sites separated by 1 bp (1–7). Ligand-receptor interactions induce conformational changes that facilitate recruitment of coactivator and coregulatory proteins required for transactivation.

PPARγ is widely expressed in cancer cell lines from multiple tumors (8–27), and a recent clinical study reported PPARγ mRNA expression in tumors from breast, lung, colon, prostate, osteosarcomas, acute myelogenous leukemia, adult T-cell leukemia, glioblastomas, B-cell acute lymphoblastic leukemia, non-Hodgkin's lymphoma, and myelodisplastic syndrome (28). PPARγ ligands such as 15-deoxy-Δ12,14-prostaglandin J2 (PGJ2) and synthetic thiazolidinediones inhibit growth of cancer cell lines, and this has been associated with modulation of multiple cell context-dependent pathways including inhibition of G$_0$/G$_1$-S phase cell cycle progression, down-regulation of cyclin D1, enhanced expression of p21 or p27 cyclin-dependent kinase inhibitors, and induction of apoptosis (8–27).

Research in this laboratory has investigated inhibitory cross-talk between the aryl hydrocarbon receptor (AhR) and estrogen receptor (ER) α signaling pathways in breast cancer cells (29, 30). Ligands for the AhR inhibit 17β-estradiol (E2)-induced growth and gene expression in ER-positive MCF-7 cells and also block growth of hormone-dependent mammary tumors in rodent models (29–34). Diindolylmethane (DIM) and several ring-substituted DIM derivatives have been characterized as selective AhR modulators that inhibit growth of carcinogen-induced mammary tumors in rats (31–33). We have also investigated the antiestrogenic activity of methylene (C)-substituted

DIMs containing bulky aromatic substituents; these C-substituted DIMs did not activate the AhR but inhibited growth of breast cancer cells (*in vitro*) and tumors (*in vivo*; 35 and data not shown). This article reports the structure-dependent PPARγ agonist activities of DIMs containing substituted phenyl groups at the methylene carbon in MCF-7 cells, and 1,1-bis(3′-indolyl)-1-(*p*-trifluoromethylphenyl)methane (DIM-C-pPhCF$_3$) is used as a prototype for mechanistic studies. DIM-C-pPhCF$_3$ and compounds containing *p*-*t*-butyl, cyano, dimethylamino, and phenyl substituents were most active as PPARγ agonists in transactivation assays, whereas analogues containing methyl, hydrogen, methoxy, hydroxyl, or halogen groups were relatively inactive. DIM-C-pPhCF$_3$ and related compounds resemble PGJ2 in MCF-7 cells, and both PPARγ agonists induce selective recruitment of coactivators in a mammalian two-hybrid assay, inhibit G_0/G_1-S phase cell cycle progression, induce apoptosis, and activate proteasome-dependent degradation of cyclin D1 and ERα proteins.

Materials and Methods

Cells, Chemicals, and Other Materials

MCF-7 cells and 3T3-L1 preadipocytes were obtained from American Type Culture Collection (Manassas, VA). MCF-7 cells were maintained in MEM supplemented with 0.22% sodium bicarbonate, 10% fetal bovine serum (FBS), 0.011% sodium pyruvate, 0.1% glucose, 0.24% HEPES, 0.00001% insulin, and 2 ml/l antibiotic solution (Sigma Chemical Co., St. Louis, MO). Cells were grown in 150 cm^2 culture plates in an air/CO_2 (95:5) atmosphere at 37°C and passaged every 5 days. For most experiments, cells were seeded in DMEM:F12 with 5% FBS. The caspase inhibitors IETD-CHO and LEHD-CHO were purchased from Alexis Biochemicals (Carlsbad, CA). PGJ2 (PG-050) was purchased from Biomol Research Laboratories Inc. (Plymouth Meeting, PA). Rosiglitazone and troglitazone were purchased from IKT Laboratories (St. Paul, MN). MG132, calpain inhibitor II (CII), and actinomycin D were purchased from Calbiochem-Novabiochem Co. (San Diego, CA). The PPARγ antagonist *N*-(4′-aminopyridyl)-2-chloro-5-nitrobenzamide (T007) was synthesized in this laboratory and confirmed by gas chromatography-mass spectrometry. Antibodies for cyclin D1 (sc-718 and sc-246), poly(ADP-ribose) polymerase (PARP), ERα (sc-544), PPARγ (sc-7196), and Sp1 (sc-59 and sc-420) were purchased from Santa Cruz Biotechnology (Santa Cruz, CA). Horseradish peroxidase substrate for Western blot analysis was purchased from NEN Life Science Products (Boston, MA). RNase ONE, pGL2 luciferase reporter vector, cell lysis buffer, and luciferase reagent were purchased from Promega (Madison, WI), and β-galactosidase (β-gal) reagent was from Tropix (Bedford, MA). Plasmid preparation kits were purchased from Qiagen, Inc. (Santa Clarita, CA), and LipofectAMINE2000 transfection kits were obtained from Invitrogen (Carlsbad, CA). Small inhibitory RNA (siRNA) duplexes for lamin A/C (iLMN), luciferase (iGL2), and PPARγ (iPPARγ) were prepared by Dharmacon Research (Lafayette, CO) and contain the sequences listed in Table 1.

Table 1. Summary of siRNAs

Gene	siRNA duplex
iPPARγ	5′-CAG AUC CAG UGG UUG CAG AAT TT GUC UAG GUC ACC AAC GUC U-5′
iGL2	5′-CGU ACG CGG AAU ACU UCG ATT TT GCA UGC GCC UUA UGA AGC U-5′
iLMN	5′-CUG GAC UUC CAG AAG AAC ATT TT GAC CUG AAG GUC UUC UUG U-5′

The series of C-substituted DIMs used in this study were prepared using the same protocol as described previously (36) by condensation of 0.02 mol of indole with 0.01 mol of a substituted benzaldehyde at pH 2.5 in dilute aqueous acetic acid. Indole and the substituted benzaldehydes were purchased from Aldrich Chemical Co. (Milwaukee, WI). Indole and the appropriate substituted benzaldehyde were added to 50 ml of water and 0.6 ml of acetic acid at room temperature. The reaction mixture was stirred and progress of the condensation reaction was monitored by thin-layer chromatography; when 80–90% of the reaction were complete, the resulting solid was filtered and crystallized from benzene or benzene/hexane. High yields of the C-substituted DIMs were obtained (70–90%) and structures were confirmed by gas chromatography-mass spectrometry and/or nuclear magnetic resonance spectroscopy. A more extensive study on spectral properties of the C-substituted DIMs will be published separately. The compounds are light sensitive and are stored in the solid form or in Me_2SO solution in dark vials.

Cloning and Plasmid Preparation

PPRE3Luc luciferase reporter was constructed using pGL2 with a minimal TATA sequence and triple consensus PPREs. The Gal4 reporter containing 5× Gal4DBD (Gal4-Luc) was kindly provided by Dr. Marty Mayo (University of North Carolina, Chapel Hill, NC). Gal4DBD-PPARγ construct (gPPARγ) was a gift of Dr. Jennifer L. Oberfield (Glaxo Wellcome Research and Development, Research Triangle Park, NC), and PPARγ expression plasmid and pM-PPARγ coactivator-1 (PGC1) were gifts of Dr. Bruce M. Spiegelman (Harvard University, Boston, MA). The PPARγ$_2$-VP16 fusion plasmid (VP-PPARγ) contained the DEF region of PPARγ (amino acids 183–505) fused to the pVP16 expression vector and was kindly provided by Dr. Shigeaki Kato (University of Tokyo, Tokyo, Japan). The Gal4-coactivator fusion plasmids pM-AIB1, pM-steroid receptor coactivator (SRC) 1, pM-TIFII, and pM-thyroid hormone receptor-associated protein 220 (TRAP220) plasmids were also provided by Dr. Shigeaki Kato.

Transient Transfection and Luciferase Activity Assay

MCF-7 cells were seeded in 12-well plates with DMEM:F12 with 5% FBS 24 h before transfection. Various amounts of DNA [*i.e.*, Gal4Luc (0.2 μg), PPRE3Luc (0.2 μg), β-gal DNA (0.04 μg), PPARγ (0.15 μg), gPPARγ (0.03 μg), pVP-PPARγ (0.03 μg), pM-AIB1 (0.03 μg), pM-SRC1 (0.03 μg), pM-TIFII (0.03 μg), and pM-TRAP220 (0.03 μg)] were mixed with LipofectAMINE2000 reagent at a ratio of

1:3 or 1:5 (μg of DNA/μl of reagent) and added to cells following the manufacturer's instructions. After incubation for 6 h, cells were treated for 24 h in fresh media as indicated. Cells were lysed with 200 μl of 1× Reporter Lysis Buffer, and 25 μl of cell extract were subjected to luciferase and β-gal assays. Luciferase and β-gal activities were quantitated by Lumicount, and luciferase activities were normalized to β-gal activity. All experiments were repeated at least thrice for each treatment group.

iPPARγ Studies

For transfection experiments, MCF-7 cells were cultured in six-well plates in 2 ml DMEM:F12 supplemented with 5% FBS. When cells were ~50–60% confluent, siRNA duplexes and/or reporter gene constructs were transfected using OligofectAMINE reagent (Invitrogen). Based on results of previous studies (37–39), siRNAs were transfected in each well to give a final concentration of 70 nM. Cells were harvested in 48–56 h after transfection by manual scraping in 1× lysis buffer (Promega). Whole cell extracts were frozen in liquid nitrogen for 30 s, vortexed by 30 s, and centrifuged at 12,000 × *g* for 1 min to give lysates that were assayed for luciferase activity as described above. In a parallel experiment, whole cell lysates from this experiment were analyzed for PPARγ protein by Western blot analysis essentially as described (39). Relative intensities of the PPARγ protein were compared with a nonspecific band and results of three replicate studies were determined in the various treatment groups.

Cell Proliferation Assay

MCF-7 cells were seeded in DMEM:F12 with 5% FBS and treated with 1, 5, or 10 μM of either DIM-C-pPhCF$_3$, DIM-C-pPhtBu, DIM-C-pPhCN, 1,1-bis(3′-indolyl)-1-(*p*-biphenyl)methane (DIM-C-pPhC$_6$H$_5$), or solvent (Me$_2$SO) as indicated. Cell numbers were determined using a Coulter Z1 counter and results for each treatment group were determined for at least three replicate studies.

Carcinogen-Induced Rat Mammary Model

Female Sprague-Dawley rats (Harlan, Indianapolis, IN) were received at 39 days of age. At 50 days of age, each animal received 7,12-dimethylbenz(*a*)anthracene (20 mg) suspended in corn oil by gavage. Tumors developed in these animals within 30–75 days after treatment. After palpable tumors were detected (250–400 mm^3), rats were treated with corn oil vehicle control (4 ml/kg) or DIM-pPhC$_6$H$_5$ (1 mg/kg) in corn oil (4 ml/kg) every second day as described (31–33). Tumor volumes were measured throughout the experiment and were calculated as $\pi \times L/2 \times W/2 \times D/2$. On day 21 (2 days after the final dose), animals were sacrificed by CO_2 asphyxiation followed rapidly by cervical dislocation, and organ and body weights were determined and shown to be unchanged by the treatment (data not shown).

Fluorescence-Activated Cell Sorting Analysis

After synchronization of cells for 24 h in serum-free medium, MCF-7 cells were treated for 20 h with different concentrations of DIM-C-pPhCF$_3$. Cells were then trypsinized, syringed, and collected by centrifugation. Single cell suspensions were prepared by resuspending cell pellets in 1× staining solution [50 μg/ml propidium iodide, 30 units/ml RNase ONE, 4 mM sodium citrate, and Triton X-100 (pH 7.8)]. Cells were incubated at 37°C for 10 min, and sodium chloride solution was added to the final concentration of 0.15 M. Stained cells were analyzed on a FACSCalibur Flow Cytometer (Becton Dickinson Immunocytometry Systems, San Jose, CA) using Cell Quest (Becton Dickinson Immunocytometry Systems) acquisition software as described (35).

Differentiation and Oil Red O Staining

3T3-L1 preadipocytes were cultured on poly-lysine-coated coverslips with DMEM and 10% FBS at 5% CO_2 in 24-well plates. At 2 days postconfluence, cells were incubated with fresh media supplemented with 3-isobutyl-1-methylxanthine (0.5 mM), dexamethasone (1 μM), insulin (1.7 μM), and PGJ2 or DIM-C-pPhCF$_3$ (1 μM). After 48 h, cells were changed to fresh media and treated with Me$_2$SO, PGJ2 (1 μM), or DIM-C-pPhCF$_3$ for 5 days. Cells without any treatment for the entire 7 days were used as control. The cells were then fixed with 10% formalin. Fixed cells were washed with 60% isopropanol and stained with filtered 60% Oil Red O in deionized water. After staining, cells were washed with water and photographed.

Western Blot Analysis

Whole cell lysates were extracted using 1× Western sampling buffer. Protein samples were heated at 100°C for 5 min, separated on 10% SDS-PAGE and transferred to polyvinylidene difluoride (PVDF) membrane (Amersham Pharmacia Biotech, Piscataway, NJ). The PVDF membrane was blocked for 1 h and incubated with 1:1000 (cyclin D1), 1:500 (PPARγ), or 1:2000 (Sp1) primary antibody (Santa Cruz Biotechnology) for 1 h or with 1:500 (ERα) for 3 h. After vigorous washing for 30 min, 1:2000 secondary antibody was incubated with shaking for 1 h. The membrane was washed for 30 min, incubated with enhanced chemiluminescence substrate (NEN Life Science Products) for 1.0 min, and exposed to Kodak X-Omat AR autoradiography film (Rochester, NY). The membrane was reused and probed with other antibodies as indicated for individual experiments.

Apoptosis Assays

MCF-7 cells (10^6) were plated in 145 mm dishes and treated with DIM-C-pPhC$_6$H$_5$ or Me$_2$SO (0.2%) for the indicated times. Floating and adherent cells were collected and resuspended in 100 μl of TE buffer (pH 8.0) and transferred to prechilled 2 ml epitubes and incubated on ice for 5 min. The cell suspension was then mixed with 500 μl of sonication buffer [1% SDS, 10 mM Tris-HCl, 1 mM EDTA (pH 8.0)] and incubated on ice for an additional 20 min. After several extractions with phenol/chloroform/isoamyl alcohol (25:24:1), 0.5 volume of sodium chloride (5 M) and 2.5 volumes of 95% ethanol were added to the aqueous layer and nucleic acids were precipitated at −20°C overnight and collected by centrifugation at 12,000 × *g* for 30 min. The pellet was washed with 80% ethanol, air dried, and resuspended in TE buffer with DNase-free RNase A (40 μg/ml) and incubated at 37°C for 2 h. DNA was run in 2% agarose gels and visualized by ethidium bromide staining. For studies on PARP cleavage, whole cell lysates from treated cells were electrophoresed in 10%

SDS-PAGE gels, and proteins were transferred to PVDF membranes (Immobilon-P; Millipore, Bedford, MA). Anti-PARP mouse monoclonal antibody (F-2; Santa Cruz Biotechnology) was incubated at 1:400 dilution at room temperature for 2 h in 1× PBS with 0.04% Tween 20. Bound antibodies were detected with horseradish peroxidase-conjugated donkey anti-mouse IgG and luminol regent (Santa Cruz Biotechnology). z-VAD-fmk, a broad-spectrum, irreversible caspase inhibitor (Santa Cruz Biotechnology), was used at a final concentration of 100 μM for determining effects of DIM-C-pPhCF$_3$ (7.5 μM) on inducing apoptotic detached MCF-7 cells after treatment for 16 h.

Physicochemical Calculations

The 2.3 Å resolution crystal structure of the ligand binding domain (residues 206–477) from human PPARγ derived from the liganded PPARγ LBD/RXRα LBD heterodimer complexed with GW409544, 9-*cis*-retinoic acid, and two LxxLL peptides from SRC1 has been published (40). The atomic coordinates and structure factors were downloaded from the Protein Data Bank (PDB; http://www.rcsb.org; PDB identification code: 1K74). RXRα, GW409544, 9-*cis*-retinoic acid, and the two peptides from SRC1 were deleted leaving the coordinates for the subunit PPARγ. DIM-C-pPhCF$_3$ and PGJ2 were created in ISIS/Draw and were energy minimized using semi-empirical quantum mechanical AM1 methods (HyperChem, Ottawa, ON, Canada). This file was converted to a PDB file by HyperChem and inserted into the Y-shaped ligand binding pocket of the crystal structure subunit of PPARγ using Swiss PDB Deep Viewer v3.7b2 from Glaxo Wellcome Experimental Research (Geneva, Switzerland). Quantitative structure-activity relationships were computed using HyperChem for DIM-C-pPhCF$_3$ and PGJ2.

Statistical Analysis

Statistical differences between different groups were determined by ANOVA and Scheffe's test for significance. Data are presented as means ± SD for at least three separate determinations for each treatment.

Results

1,1-Bis(3′-Indolyl)-1-(*p*-Substituted Phenyl)Methanes as PPARγ Agonists in Transactivation and Adipocyte Differentiation Assays

Ring-substituted DIMs activate the AhR and inhibit E2-induced growth of breast cancer *in vitro* and mammary tumor growth in carcinogen-induced female Sprague-Dawley rats (31–33). In contrast, a series of C-substituted DIMs, which did not activate the AhR, also inhibited breast cancer cell growth. These lipophilic compounds, typified by DIM-C-pPhCF$_3$, were systematically investigated in transactivation assays as ligands for other receptors, including PPARγ, PPARα, retinoic acid receptor (RAR), and RXR. PGJ2, DIM-C-pPhCF$_3$, and isomers with *o*- and *m*-trifluoromethyl groups induced luciferase activity in MCF-7 cells transfected with PPRE3Luc/PPARγ expression plasmid (Fig. 1A). PGJ2 and DIM-C-pPhCF$_3$ (10 and 20 μM) induced luciferase activity in both assays, whereas *o*-CF$_3$ and *m*-CF$_3$ analogues were less active at the 20 μM concentration. Comparable results were obtained in cells transfected with Gal4Luc/PPARγ. DIM-C-pPhCF$_3$ did not induce transactivation in MCF-7 cells using Gal4Luc and Gal4-receptor chimeras containing PPARα, RXR, or RAR, and activation of AhR- and ERα-mediated responses were also not observed (data not shown).

Thiazolidinediones such as rosiglitazone and troglitazone are synthetic PPARγ agonists that have been extensively investigated. Results in Fig. 1B compare concentration-dependent activation of PPARγ by DIM-C-pPhCF$_3$ (-CF$_3$) and DIM-C-pPhtBu (-tBut) and the thiazolidinediones in MCF-7 cells transfected with Gal4-luc/pM-PPARγ. DIM-C-pPhCF$_3$ and DIM-C-pPhtBu (5–10 μM) induced a maximal 5.5–6.5-fold response, and this decreased at higher concentrations due to cytotoxicity. Rosiglitazone and troglitazone induced transactivation in MCF-7 cells at lower concentrations; however, the maximum fold induction (4–5-fold) was lower than observed for the C-substituted DIMs. This was consistently observed in replicate experiments.

The effects of substituent structure on the activity of a series of 1,1-bis(3′-indolyl)-1-(*p*-substituted phenyl)methane analogues was also investigated in PPARγ-mediated transactivation assays (Fig. 1, C and D), which gave complementary results. At concentrations of 10 or 20 μM, the most active compounds contained the *p*-CF$_3$, *p*-*t*-butyl, *p*-cyano, *p*-phenyl (C$_6$H$_5$), or *p*-dimethylamino substituents. Higher concentrations of these compounds were cytotoxic. In contrast, minimal to nondetectable responses were observed after treatment of MCF-7 cells with 10 or 20 μM concentrations of compounds containing *p*-hydrogen, hydroxyl, fluoro, bromo, methoxy, or methyl substituents.

Recent studies identified T007 as a PPARγ antagonist that inhibited thiazolidinedione-induced transactivation in HEK 293 cells and adipocyte differentiation in 3T3-L1 cells (41). In this study, T007 also inhibited activation of PPARγ by PGJ2 and DIM-C-pPhCF$_3$ in MCF-7 cells transfected with Gal4Luc/pM-PPARγ or PPARE3Luc/PPARγ expression plasmid (Fig. 2, A and B). In contrast, T007 (20 μM) alone did not significantly inhibit activity in cells transfected with Gal4Luc/pM-PPARγ, whereas inhibition (40%) was observed in cells transfected with PPRE3Luc/PPARγ expression plasmid (data not shown). T007 (20 μM) inhibited ~50% of PGJ2 (20 μM)-induced transactivation in both assays, whereas a higher percentage of inhibition of DIM-C-pPhCF$_3$-induced activity was observed. This was particularly evident for the Gal4Luc/pM-PPARγ assay where T007 (0.2 μM) inhibited 80% of DIM-C-pPhCF$_3$-induced transactivation. In parallel studies, we also used iPPARγ in an RNA interference assay, and results in Fig. 2C show that in MCF-7 cells transfected with iPPARγ, there was a significant decrease in PPARγ protein as determined by Western blot analysis of whole cell lysates. In two separate experiments, iPPARγ inhibited PGJ2 (Fig. 2D)- and DIM-C-pPhCF$_3$ (Fig. 2E)-induced luciferase activity in MCF-7 cells transfected with PPARE3Luc compared with cells treated with iLMN (a siRNA targeted

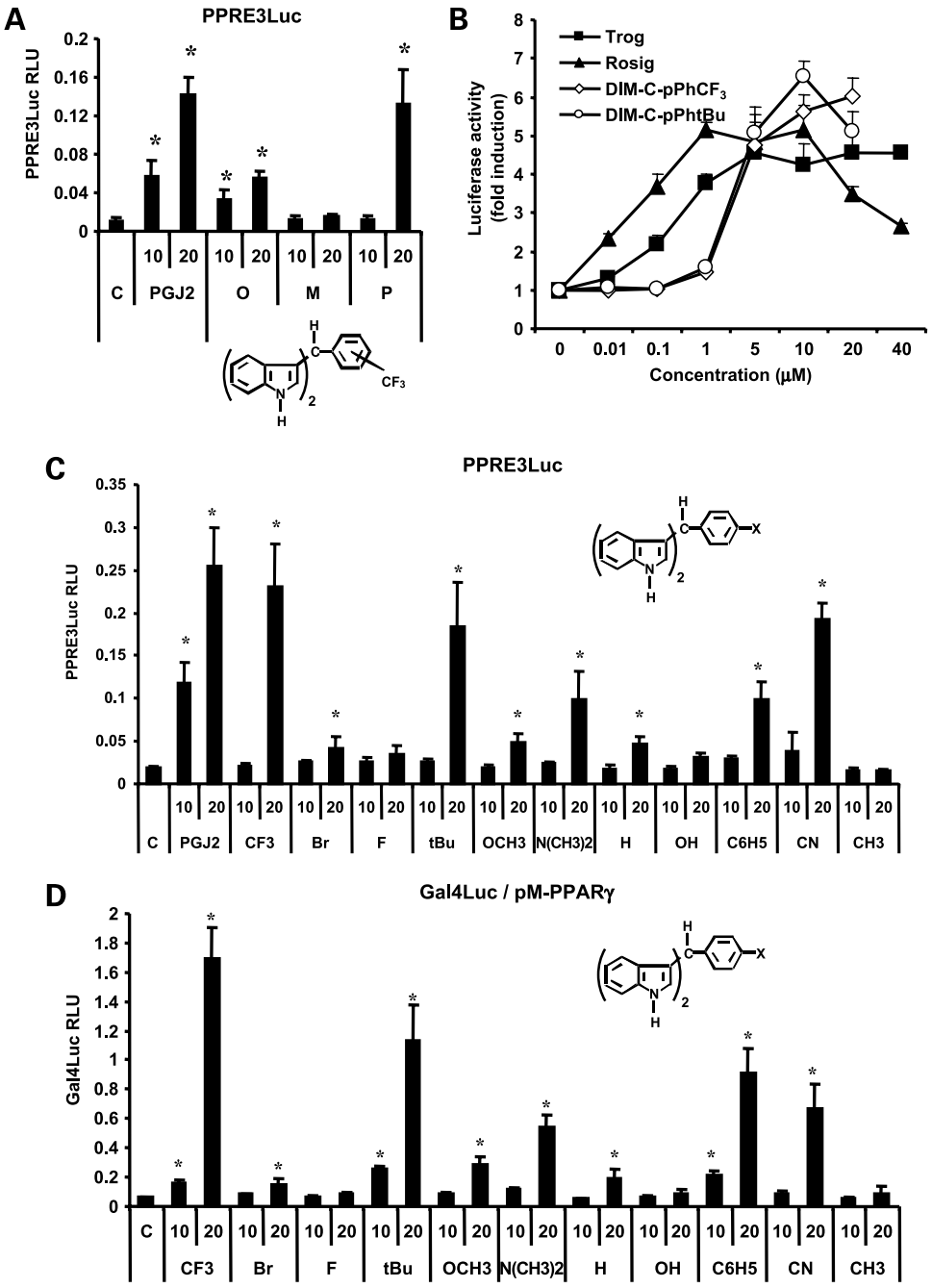

Figure 1. Induction of PPARγ-dependent transactivation by PGJ2 and 1,1-bis(3′-indolyl)-1-(*p*-substituted phenyl) methanes. **A,** activation of PPRE3Luc by PGJ2 and C-substituted DIMs. MCF-7 cells were transfected with PPRE3Luc/PPARγ or Gal4-Luc/pM-PPARγ constructs and treated with Me_2SO (*C*) or different concentrations of the compounds (as indicated) and luciferase activities were determined as described in Materials and Methods. **B,** activation of Gal4Luc/pM-PPARγ. MCF-7 cells were transfected with Gal4Luc/pM-PPARγ and treated with different concentrations of DIM-C-pPhCF$_3$ (*CF3*), DIM-C-pPhtBu (*tBu*), troglitazone (*Trog*), or rosiglitazone (*Rosig*) and luciferase activity was determined as described in Materials and Methods. Activation of PPRE3Luc/PPARγ (**C**) or Gal4Luc/pM-PPARγ (**D**) by PGJ2 or 1,1-bis(3′-indolyl)-1-(*p*-substituted phenyl)methanes. MCF-7 cells were treated as described above (**A** or **B**). *Columns,* means for three replicate experiments for each treatment group; *bars,* SD. *, $P < 0.05$, significant induction over the Me_2SO control (*C*).

to lamin A/C). iGL2, which targets the bacterial luciferase mRNA, also decreased activity in cells treated with Me_2SO or PPARγ agonist. In contrast, iPPARγ did not affect induction of luciferase activity in MCF-7 cells treated with E2 (10 nM) and transfected with an E2-responsive pERE$_3$ construct (data not shown). Thus, both iPPARγ and T007, a PPARγ antagonist, inhibited PGJ2- and DIM-C-pPhCF$_3$-mediated transactivation.

PPARγ agonists characteristically induce cellular differentiation in 3T3-L1 adipocytes, and this is characterized by altered gene expression and accumulation of fat droplets, which can be detected by Oil Red O staining. Results in Fig. 3 show that in control 3T3-L1 cells and after treatment with Me_2SO, PGJ2 (1 μM), and DIM-C-pPhCF$_3$ (1 μM), a significant increase in Oil Red O staining of fat droplets was only observed in the latter two treatment groups. Thus, DIM-C-pPhCF$_3$, like PGJ2 and other synthetic PPARγ agonists, induced PPARγ-dependent differentiation in 3T3-L1 cells.

Ligand Structure-Dependent Interactions of PPARγ and Coactivators

Ligand-induced transactivation mediated by PPARγ and other NHRs is dependent on recruitment of coactivator proteins. These include SRCs (42), mediator complex (43–46) proteins such as PBP/TRAP220/DRIP 205 (45),

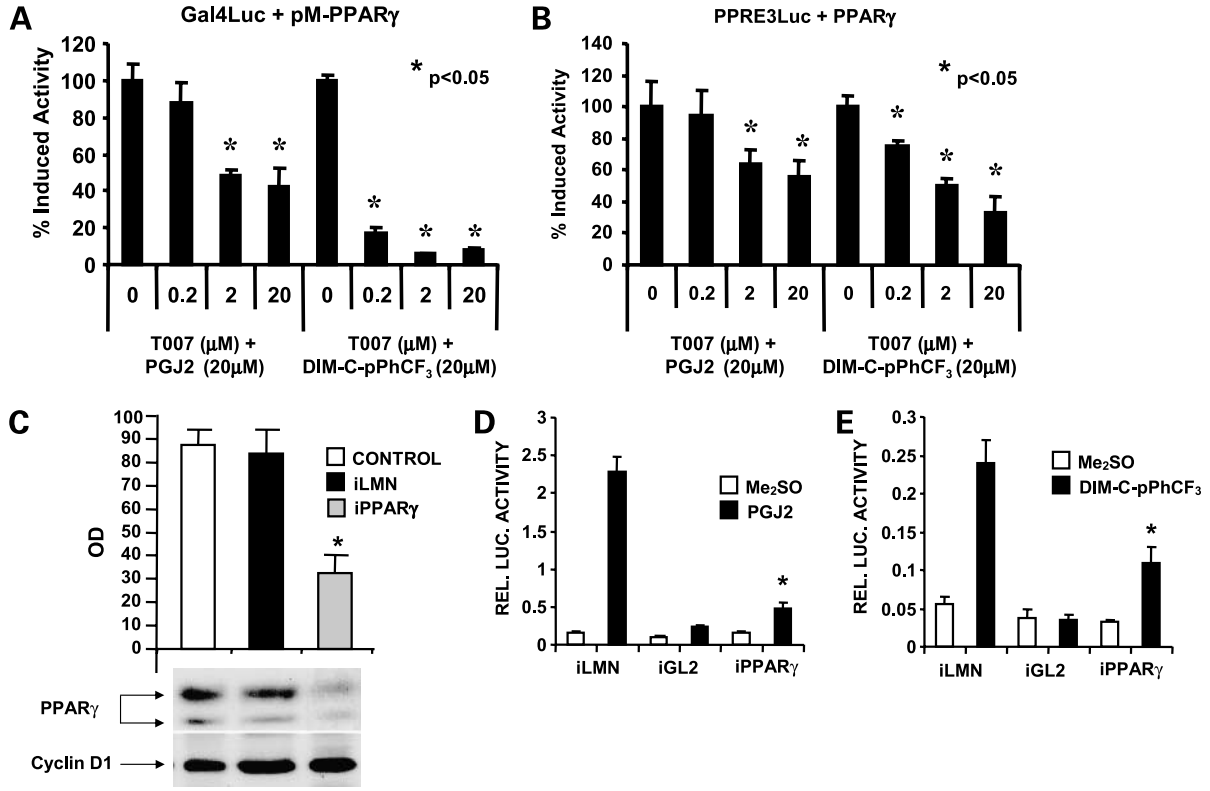

Figure 2. Inhibition of PPARγ-dependent transactivation by T007. Inhibitory effects of T007 in cells transfected with Gal4Luc (**A**) or PPRE3Luc (**B**). MCF-7 cells were treated with different concentrations of T007 plus PGJ2 (20 μM) or DIM-C-pPhCF$_3$ (20 μM) transfected with Gal4Luc/pM-PPARγ (**A**) or PPRE3Luc/PPARγ (**B**) and luciferase activities were determined as described in Materials and Methods. *Columns,* means for three replicate determinations for each treatment group; *bars,* SD. *, $P < 0.05$, significant inhibition by T007. In cells transfected with Gal4Luc/pM-PPARγ, T007 (20 μM) did not significantly decrease activity in solvent (Me_2SO)-treated cells, whereas a 40% decrease was observed in cells transfected with PPRE3Luc/PPARγ (data not shown). **C,** down-regulation of PPARγ protein. MCF-7 cells were transfected with iPPARγ, iLMN, or untreated (*CONTROL*) and whole cell lysates were examined by Western blot analysis as described in Materials and Methods. *Columns,* relative intensities of the PPARγ protein bands from three replicate experiments; *bars,* SD. *, $P < 0.05$, significantly decreased band intensities observed only in cells transfected with iPPARγ. Effects of iPPARγ on PGJ2- (**D**) and DIM-C-pPhCF$_3$- (**E**) induced activity. Cells were transfected with PPARE3Luc and iLMN, iGL2, or iPPARγ and treated with Me_2SO and PGJ2 (**D**) or DIM-C-pPhCF$_3$ (**E**) and luciferase activity was determined as described in Materials and Methods. *Columns,* means for three replicate determinations; *bars,* SD. *, $P < 0.05$, significant inhibition by iPPARγ.

and PGC1 (47–53). Results in Fig. 4 summarize ligand-dependent transactivation in MCF-7 cells transfected with pM-coactivator and VP-PPARγ chimeric expression plasmids and a Gal4Luc reporter construct. This mammalian two-hybrid assay determines the effects of PPARγ agonists to induce conformational changes in the ligand binding domain, which are required for subsequent binding to coactivators. The pattern of activation by PGJ2 and DIM-C-pPhCF$_3$ exhibited both similarities and differences. Both PPARγ ligands activated gene expression in MCF-7 cells transfected with pM-SRC1 and pM-TIFII (SRC2) but not pM-AIB1 (SRC3). DIM-C-pPhCF$_3$ (1–10 μM) induced transactivation in cells transfected with pM-TRAP220, whereas only a submaximal response was observed for PGJ2 (2.5 μM). In contrast, previous studies showed that PGJ2 induced activity in COS-1 cells transfected with VP-PPARγ and chimeric SRC1, TIFII, AIB1, and TRAP220-Gal4 proteins (54). The major difference between PGJ2 and C-substituted DIMs in the mammalian two-hybrid assay in MCF-7 cells was observed using PGC1. Both DIM-C-pPhCF$_3$ and DIM-C-pPhC$_6$H$_5$ induced interactions between PPARγ and PGC1, whereas treatment with PGJ2 decreased activity. These results further demonstrate that C-substituted DIMs induce interactions between PPARγ and coactivators, which is characteristic of PPARγ agonists.

Inhibition of Breast Cancer Cell Growth and Mammary Tumor Growth by 1,1-Bis(3′-Indolyl)-1-(*p*-Substituted Phenyl)Methanes

PPARγ agonists typically inhibit growth of breast cancer cells (22, 24, 25, 35), and results in Fig. 5 illustrate the effects of 1,1-bis(3′-indolyl)-1-(*p*-substituted phenyl) methane analogues (1, 5, and 10 μM) as inhibitors of MCF-7 cell growth. These compounds contain *p*-trifluoromethyl, *p*-phenyl (C$_6$H$_5$), *p*-*t*-butyl, and *p*-cyano substituents on the phenyl ring and were among the most active PPAR agonists in the screening assay (Fig. 1). Significant inhibition of MCF-7 cell growth was observed at concentrations of ≥ 1 μM and the higher concentrations (5 and/or 10 μM) were cytotoxic; cell numbers after treatment with cytotoxic doses were lower than the number of attached cells on day 1, and floating dead cells were observed. The effects of DIM-C-pPhCF$_3$ on

MCF-7 cell cycle progression was investigated by fluorescence-activated cell sorting (FACS) analysis after treatment with DIM (10 or 30 μM) for 20 h. The percentage of cells in G_0/G_1 after treatment with Me_2SO, DIM-C-pPhCF$_3$ (10 μM) and DIM-C-pPhCF$_3$ (30 μM) was 56.5%, 76.6%, and 90.8%, respectively, and the percentage in S phase was 43.2%, 23.1%, and 9.0%, respectively (Fig. 5E). Thus, DIM-C-pPhCF$_3$ inhibited G_0/G_1-S phase progression of MCF-7 cells, and this is consistent with previous studies on the effects of PGJ2 in MCF-7 cells (35). One of these compounds (DIM-C-pPhC$_6$H$_5$) was also investigated as a mammary tumor growth inhibitor in 7,12-dimethylbenz(*a*)anthracene-induced female Sprague-Dawley rats, and significant ($P < 0.05$) inhibition was observed at a dose of 1.0 mg/kg every second day (×10; Fig. 5F). Ongoing studies in rodents with C-substituted DIMs and ring-substituted DIMs (31–33) indicated that total doses as high as 300 mg/kg did not cause changes in body or organ weights or organ histopathology. This compound was selected for the initial *in vivo* studies due to its activity as a PPARγ agonist (Fig. 1) and chemical stability (resistance to photodegradation). Inhibition of breast cancer cell growth, decreased G_0/G_1-S phase progression, and tumor growth inhibition by C-substituted DIMs are consistent with their activity as PPARγ agonists in mammary cancer cells.

Effects of C-Substituted DIMs on Apoptosis

Treatment of MCF-7 cells with Me_2SO or different concentrations of DIM-C-pPhC$_6$H$_5$ shows that the growth inhibitory effects of this compound (Fig. 6) are accompanied by apoptosis. PARP is a substrate for activated caspases (55), and incubation of MCF-7 cells for 36 h with DIM-C-pPhC$_6$H$_5$ (5 or 10 μM) induced cleavage of PARP to give the characteristic 85-kDa degradation product (Fig. 6A). Results in Fig. 6B show that DIM-C-pPhC$_6$H$_5$ (10 μM)-induced cleavage of PARP was not inhibited by IETD-CHO (20 μM) or LEHD-CHO (20 μM), which specifically inhibit the apical caspase-8 and caspase-9, respectively. The same concentrations of caspase inhibitors block cycloheximide (CHX)- and MG132-induced cleavage of PARP in MCF-7 cells. Both of these compounds induce apoptosis and activation of caspase-8 and caspase-9 (56, 57). Results indicate that DIM-C-pPhC$_6$H$_5$-induced cleavage of PARP was not dependent on activation of caspase-8 or caspase-9. Induction of PARP cleavage by DIM-C-pPhC$_6$H$_5$ was also accompanied by increased DNA laddering (Fig. 6C), and the pan-caspase inhibitor z-VAD-fmk significantly protected from DIM-C-pPhC$_6$H$_5$-induced PARP cleavage (data not shown) and cell detachment (Fig. 6D; 58, 59). Inhibition of DIM-C-pPhC$_6$H$_5$-induced apoptosis by T007, and structurally related PPARγ antagonists gave inconclusive results because the compounds alone induced apoptosis (data not shown). Results demonstrate that C-substituted DIMs induce apoptosis in MCF-7 cells and this response is typically observed for PPARγ agonists in other cancer cell lines (reviewed in 4–6).

Effects of C-Substituted DIMs on Degradation of Cyclin D1 and ERα Protein in MCF-7 Cells

Treatment of MCF-7 cells with PGJ2 and ciglitazone inhibited G_0/G_1-S phase progression, and this was accompanied by decreased expression of cyclin D1 and ERα proteins through activation of proteasomes (35). Results in Fig. 7A show that both PGJ2 and DIM-C-pPhCF$_3$ induce a concentration-dependent decrease in cyclin D1 and ERα protein expression in whole cell extracts after treatment with both compounds for 8 h. Decreased levels of cyclin D1 and ERα proteins were observed in cells treated with DIM-C-pPhCF$_3$ (concentrations between 10 and 20 μM), whereas levels of immunoreactive PPARγ and Sp1 proteins were unchanged (Fig. 7A). In contrast, levels of other cell cycle regulatory proteins including cyclin A, cyclin E, p21, and p27 were unaffected by this treatment. A time course study

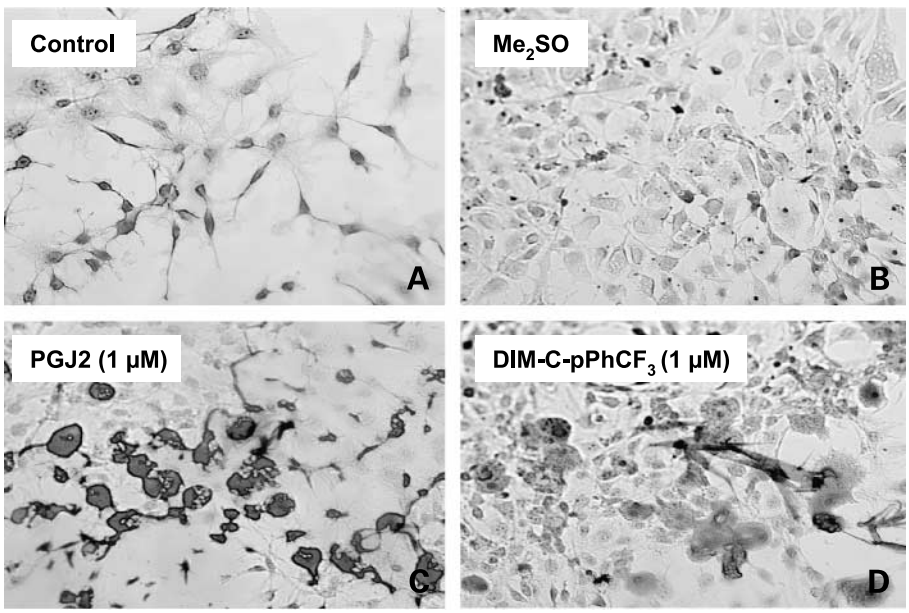

Figure 3. Enhanced Oil Red O staining in 3T3-L1 cells. Controls (**A**) and Me_2SO- (**B**), PGJ2- (1 μM; **C**), and DIM-C-pPhCF$_3$- (1 μM; **D**) treated 3T3-L1 cells were cultured and stained with Oil Red O as described in Materials and Methods. Enhanced staining of lipid droplets in cells treated with PGJ2 or DIM-C-pPhCF$_3$ was observed in multiple experiments using different concentrations (1 – 5 μM) of both compounds.

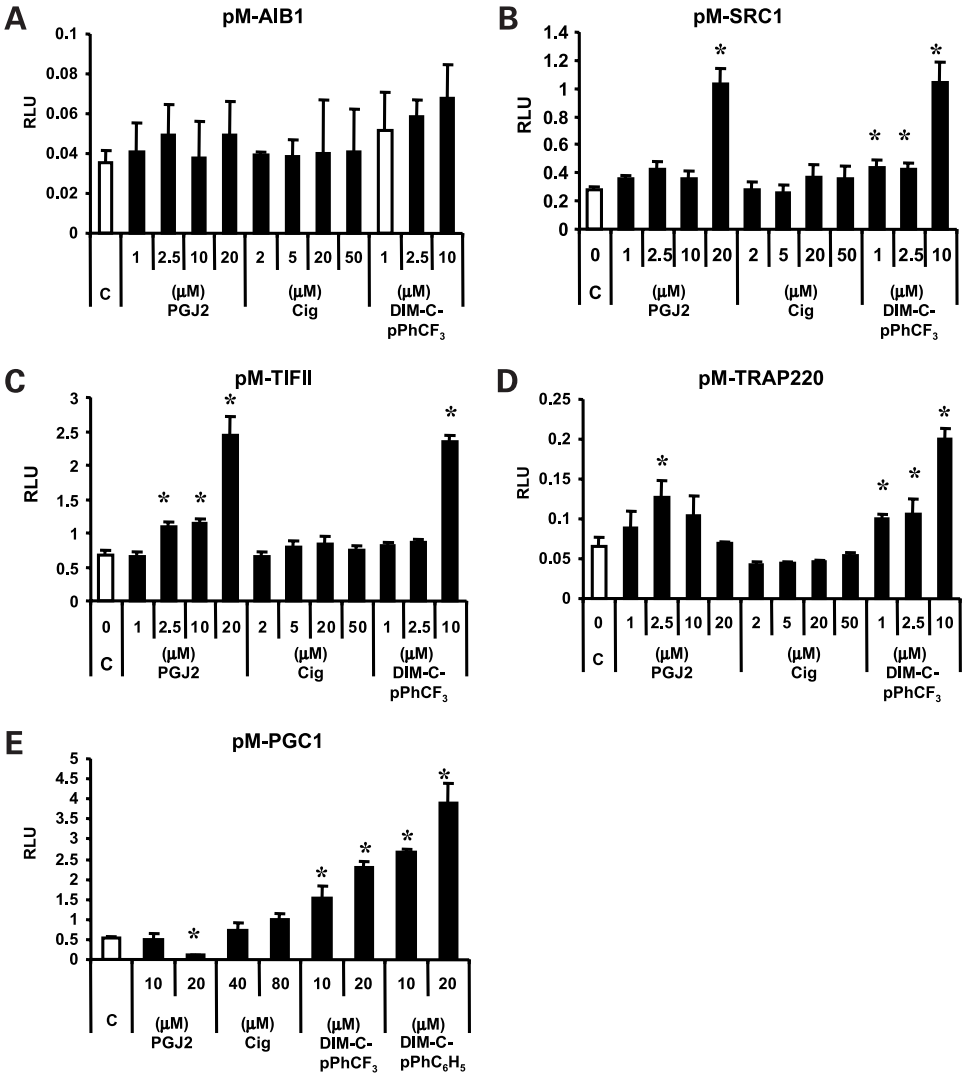

Figure 4. Ligand-dependent interactions of coactivators and PPARγ in a mammalian two-hybrid assay. MCF-7 cells were transfected with pM-AIB1 (**A**), pM-SRC1 (**B**), pM-TIFII (**C**), pM-TRAP220 (**D**), or PGC1 (**E**). MCF-7 cells were cotransfected with pM-coactivators/Gal4Luc/VP-PPARγ and treated with Me_2SO (*C*), PGJ2 (1 – 20 μM), ciglitazone (2 – 50 μM; *Cig*), or DIM-C-$pPhCF_3$/DIM-C-$pPhC_6H_5$ (up to 20 μM) and luciferase activity was determined as described in Materials and Methods. *Columns,* means for three replicate experiments for each treatment group; *bars,* SD. *, $P < 0.05$, significant induction over the Me_2SO control (*C*).

using relatively high concentrations of PGJ2 (30 μM) and DIM-C-$pPhCF_3$ (30 μM; Fig. 7B) showed that cyclin D1 and ERα protein levels are decreased as early as 1–3 and 3–15 h after treatment with the PPARγ agonists, respectively. Treatment of MCF-7 cells for a longer time period (20 h) showed that DIM-C-$pPhCF_3$-induced degradation of cyclin D1 and ERα was observed at concentrations of 10–12.5 μM (Fig. 7C). Results in Fig. 7D show that PGJ2-induced down-regulation of cyclin D1 and ERα was blocked by the proteasome inhibitor MG132 but not by the protease inhibitor CII (Fig. 7D). Similar results were observed in MCF-7 cells cotreated with DIM-C-$pPhCF_3$ plus these inhibitors, whereas in solvent (Me_2SO)-treated cells, MG132 and CII had minimal effects on ERα and cyclin D1 levels. These studies used the short time period (8 h) and higher concentrations of PGJ2 (30 μM) and DIM-C-$pPhCF_3$ (30 μM) because MG132 is cytotoxic after incubation for longer time periods. Thus, both PGJ2 and DIM-C-$pPhCF_3$ induced proteasome-dependent degradation of ERα and cyclin D1 in MCF-7 cells, and this was also observed in a recent study with ciglitazone and PGJ2 (35).

There are several possible mechanisms of PGJ2-induced down-regulation of cyclin D1, and these include PPARγ-independent pathways such as those observed for cyclopentenone, prostaglandin A2, and PGJ2 in breast cancer cells (60–62). Treatment of MCF-7 cells with PGJ2 (15 μM) alone or after cotreatment with actinomycin D (0.5 or 5.0 μM; Fig. 7E) resulted in decreased cyclin D1 and ERα protein levels, and similar results were observed for DIM-C-$pPhCF_3$ (data not shown). These data suggest a post-transcriptional mechanism of PGJ2-induced down-regulation of cyclin D1 and ERα and do not exclude the reported PPARγ-dependent competition for limiting levels of p300 as a mechanism for repression of cyclin D1 (25). However, results illustrated in Fig. 7F show that the PPARγ inhibitor T007 did not block down-regulation of cyclin D1 or ERα in cells treated with DIM-C-$pPhCF_3$ or PGJ2, suggesting that both compounds act through PPARγ-independent pathways.

The functional similarities between DIM-C-$pPhCF_3$ and PGJ2 were investigated by comparing their physical properties using HyperChem and by showing their

interactions with the ligand binding domain of PPARγ (7, 40) using atomic coordinates downloaded from the PDB. Although the surface areas of DIM-C-pPhCF$_3$ (440.96 Å^2) and PGJ2 (689.87 Å^2) were different, their atomic volumes (1028.83 and 1096.81 Å^3, respectively) and octanol/water partition coefficients (log P = 5.30 and 5.30, respectively) showed minimal differences. Both DIM-C-pPhCF$_3$ and PGJ2 are readily accommodated by the Y-shaped ligand binding pocket of PPARγ. Future studies will investigate interactions of this new class of PPARγ agonists using X-ray crystallography to further define the overall structure of the ligand-bound complex and design new structurally related PPARγ agonists.

Discussion

DIM is a metabolite of indole-3-carbinol, a phytochemical that contributes to the anticarcinogenic activity of cruciferous vegetables (63–66). DIM and related compounds bind the AhR (67), and research in this laboratory has characterized inhibitory AhR-ERα cross-talk in breast cancer cells and the anticarcinogenic activities of DIM and several ring-substituted DIMs in the rat mammary tumor model (31–34). Various acid-catalyzed condensation products derived from indole-3-carbinol bind the AhR and ERα (31–34, 67–69), and other structurally diverse indoles exhibit activities as cancer cell growth inhibitors, tubulin inhibitors, kinase inhibitors, and ligands for other receptors (70–75). For example, substituted 2-arylindoles bind the human neurokinin-1 receptor (74) and substituted indole-5-carboxylic acids activate PPARγ (75).

Introduction of a bulky substituted phenyl group on the methylene bridge of DIM eliminated the AhR agonist activity of these compounds in transactivation assays (data not shown). However, like DIM/ring-substituted DIMs, the C-substituted phenyl analogues inhibited growth of MCF-7 cells (Fig. 5); DIM-C-pPhC$_6$H$_5$ also inhibited MCF-7 cell proliferation and growth of carcinogen-induced mammary tumors in female Sprague-Dawley rats (Fig. 5).

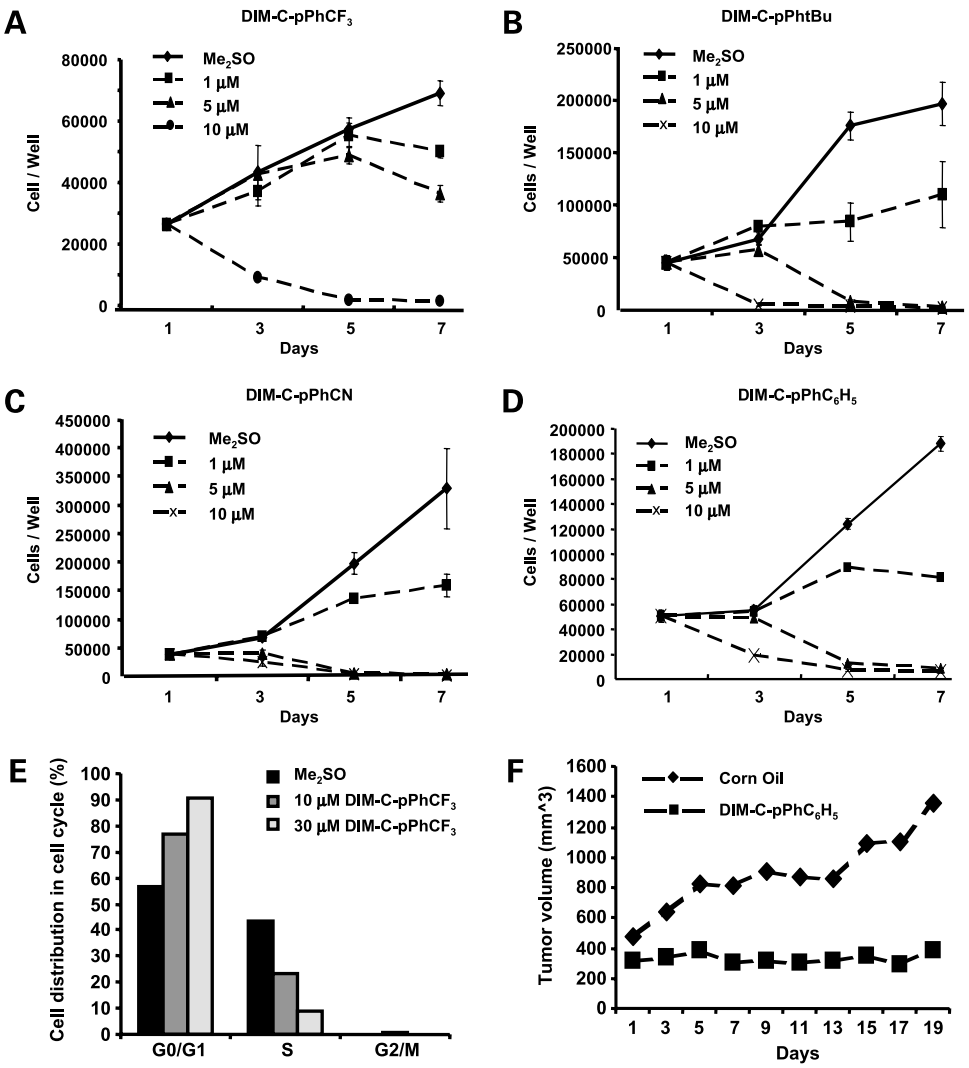

Figure 5. Inhibition of breast cancer cell and tumor growth by selected 1,1-bis(3′-indolyl)-1-(*p*-substituted phenyl)methanes. Inhibition of MCF-7 cell growth by DIM-C-pPhCF$_3$ (**A**), DIM-C-pPhtBu (**B**), DIM-C-pPhCN (**C**), and DIM-C-pPhC$_6$H$_5$ (**D**). MCF-7 cells were seeded in 24-well plates and treated with 1, 5, or 10 μM of the different compounds and cell numbers were determined after 7 days as described in Materials and Methods. **E,** cell cycle progression. MCF-7 cells were synchronized in serum-free media for 24 h and treated with Me$_2$SO and DIM-C-pPhCF$_3$ (10 and 30 μM) for 20 h in DMEM:F12 with 5% FBS, and the percentage distribution of cells in G$_0$/G$_1$, S, and G$_2$/M was determined by FACS analysis and propidium iodide staining as described in Materials and Methods. Similar results were obtained in duplicate experiments. **F,** tumor growth inhibition. The effects of DIM-C-pPhC$_6$H$_5$ (1 mg/kg) on growth of carcinogen-induced mammary tumors in female Sprague-Dawley rats were determined as described in Materials and Methods. Significant inhibition of tumor growth was observed ($P < 0.05$).

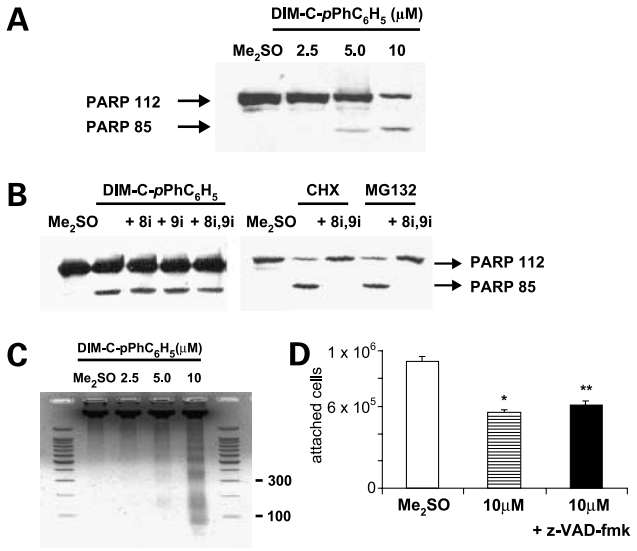

Figure 6. DIM-C-pPhC$_6$H$_5$ induced apoptosis in MCF-7 cells. **A,** PARP cleavage. Cell lysates were prepared as described in Materials and Methods and proteins were subjected to SDS-PAGE and immunoblotted with an antibody that recognizes full-length PARP (112 kDa) and its caspase cleavage product (85 kDa). **B,** effects of caspase-8 and caspase-9 inhibitors on PARP cleavage. MCF-7 cells were treated with DIM-C-pPhC$_6$H$_5$ (as described above), CHX (100 μg/ml), or MG132 (15 μM) alone or in the presence of the caspase-8 inhibitor IETD-CHO (20 μM; *8i*), the caspase-9 inhibitor LEHD-CHO (20 μM; *9i*), or their combination. PARP cleavage was determined as described in Materials and Methods. **C,** DNA ladder formation. Genomic DNA was prepared as described in Materials and Methods and run on 2% agarose gels, and oligosomal DNA was visualized by ethidium bromide staining. **D,** z-VAD-fmk inhibition. MCF-7 cells were treated with compound DIM-C-pPhC$_6$H$_5$ (7.5 μM) alone and in combination with z-VAD-fmk (100 μM) for 16 h, and the attached cells were subsequently counted. *Columns,* means for three replicate determinations; *bars,* SD. *, $P < 0.05$, DIM-C-pPhC$_6$H$_5$ alone significantly decreased the number of attached cells; **, $P < 0.05$, in combination with z-VAD-fmk, this response was only slightly reversed.

Results of transactivation assays using Gal4-receptor chimeras for receptors that bind lipophilic compounds showed that DIM-C-pPhCF$_3$ activated PPARγ and not other NHRs. Structure-activity studies among a series of 1,1-bis(3′-indolyl)-1-(*p*-substituted phenyl)methane analogues identified several compounds that were PPARγ agonists. Although the *p*-substituent on the C-phenyl markedly affected transactivation, the specific molecular determinants required for maximal activity were not apparent. For example, compounds containing both electron-donating (*t*-butyl) and electron-withdrawing (CN and CF$_3$) *p*-substituents were active in transactivation assays (Fig. 1), and molecular volumes of substituents were also not predictors of activity. These results are consistent with previous studies showing that PPARγ binds structurally diverse endogenous and synthetic compounds including fatty acids, prostaglandins, flavonoids, substituted terpenoids, thiazolidinediones, and substituted L-tyrosine and L-leucine derivatives (reviewed in 1–7). Molecular modeling studies show that the physicochemical properties of DIM-C-pPhCF$_3$ and PGJ2 are similar, and both compounds interact with the ligand binding pocket of PPARγ. Compared with the synthetic thiazolidinediones, DIM-C-pPhCF$_3$ was significantly more potent as an inducer of PPARγ-dependent transactivation in MCF-7 cells (Fig. 1B).

Recent studies have demonstrated that T007 is a specific PPARγ antagonist that inhibits PPARγ-induced transactivation (41). T007 covalently interacts with Cys^{313} in helix 3 of human PPARγ and this affects the conformation of helix 12 and subsequent interactions with coactivators and coactivator-derived peptides. T007 also inhibits DIM-C-pPhCF$_3$- and PGJ2-induced transactivation in MCF-7 cells (Fig. 2), and this is consistent with the PPARγ agonist activity of PGJ2 and the new C-substituted DIMs. Moreover, using an RNA interference assay with iPPARγ, we could also show that transfected iPPARγ inhibits PGJ2- and DIM-C-pPhCF$_3$-dependent activation of PPARE3Luc via decreased expression of PPARγ protein in whole cell extracts (Fig. 2, C–E). It was reported previously that PGJ2, but not troglitazone or 9-hydroxyoctadienoic acid, induced transactivation in COS-1 cells transfected with chimeric VP-PPARγ and Gal4-SRC1, Gal4-TIFII, Gal4-AIB1, or Gal4-TRAP220 fusion proteins (54). In contrast, using the same two-hybrid assay and Gal4-coactivator constructs in MCF-7 cells, PGJ2 induced transactivation in cells transfected with Gal4-SRC1, Gal4-TIFII, and Gal4-TRAP220 (partial) but not Gal4-AIB1 (Fig. 4). Thus, PGJ2-induced coactivator-PPARγ interactions are cell context dependent, and it is noteworthy that AIB1, which is highly expressed in breast cancer cells (76–78), does not interact with VP-PPARγ in MCF-7 cells treated with PGJ2, ciglitazone (data not shown), or DIM-C-pPhCF$_3$. The major difference between PGJ2 and C-substituted DIMs was observed with PGC1 in which only the latter compounds induced PGC1-PPARγ interactions in MCF-7 cells.

PGJ2 and other PPARγ agonists typically inhibit cancer cell growth, and this is accompanied by several responses including inhibition of G$_1$-S phase progression, cyclin D1 down-regulation, and increased differentiation and/or apoptosis, and comparable responses were observed for C-substituted DIMs (8–27, 35). C-substituted DIMs inhibit MCF-7 cell proliferation, G$_1$-S phase progression, and mammary tumor growth in carcinogen-induced female Sprague-Dawley rats (Fig. 5). DIM-C-pPhC$_6$H$_5$ was among the most active compounds in the *in vitro* and *in vivo* cell proliferation assays, and results in Fig. 6 summarize the effects of DIM-C-pPhC$_6$H$_5$ on apoptosis in MCF-7 cells 36 h after treatment. Results show that caspase-dependent cleavage of PARP and DNA laddering were observed at the 5 and 10 μM concentrations of DIM-C-pPhC$_6$H$_5$, and the broad-spectrum caspase inhibitor z-VAD-fmk only slightly inhibited DIM-C-pPhC$_6$H$_5$-induced cell death. MCF-7 cells do not express caspase-3 (79, 80); however, several agents including hydrogen peroxide, tumor necrosis factor/CHX, and paclitaxel also induce PARP cleavage in MCF-7 cells (80–82). Using specific inhibitor (LEHD-CHO/IETD-CHO) and pan-caspase inhibitor (z-VAD-fmk), our results suggest that DIM-C-pPhC$_6$H$_5$-induced apoptosis is not dependent on activation of caspase-8 or caspase-9 through the death receptor or mitochondrial pathways, respectively.

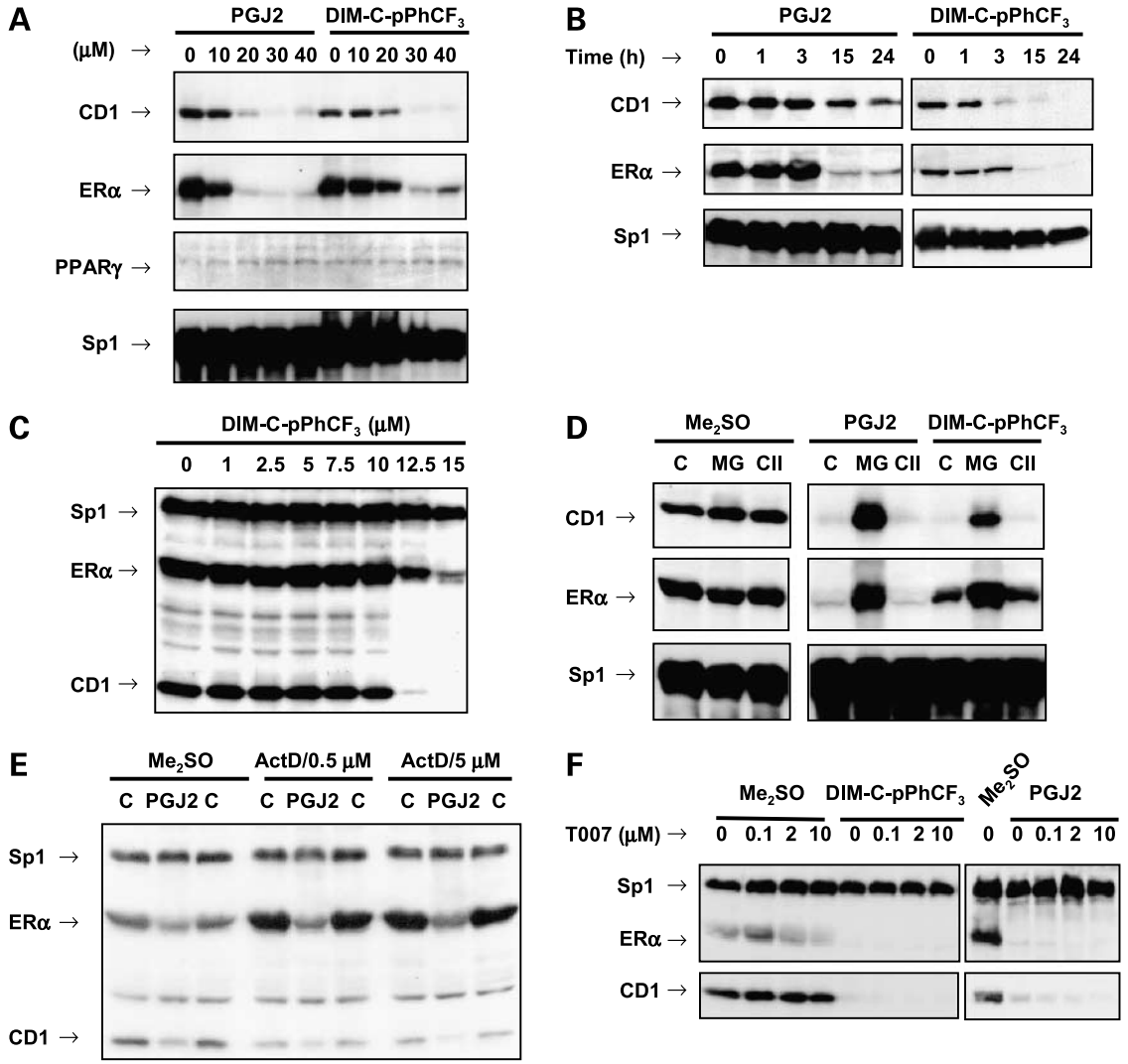

Figure 7. Comparative effects of PGJ2 and DIM-C-pPhCF$_3$ on cyclin D1 (*CD1*) and ERα protein levels in MCF-7 cells. Concentration- (**A** and **C**) and time- (**B**) dependent effects of PGJ2 and/or DIM-C-pPhCF$_3$ on cyclin D1 and ERα protein levels. MCF-7 cells were treated with different concentrations of PGJ2 or DIM-C-pPhCF$_3$ for 8 (**A**) or 20 (**C**) h or with PGJ2 (20 μM) or DIM-C-pPhCF$_3$ (20 μM) from 0 – 24 h (**B**), and protein levels were determined by immunoblot analysis of whole cell lysates as described in Materials and Methods. Sp1 protein is not significantly degraded under these treatment conditions (35) and serves as a loading control. **D,** effects of proteasome and protease inhibitors. Cells were treated with Me$_2$SO, PGJ2 (30 μM), or DIM-C-pPhCF$_3$ (30 μM) in the presence of solvent (*C*), the proteasome inhibitor MG132 (*MG*), or the protease inhibitor CII for 8 h, and whole cell lysates were analyzed by immunoblot analysis for cyclin D1, ERα, or Sp1 protein as described in Materials and Methods. Results obtained in **A** – **D** were observed in duplicate experiments. **E,** effects of actinomycin D (*ActD*) on PGJ2-induced degradation of cyclin D1 and ERα. Cells were treated with PGJ2 (15 μM) or solvent (*C*) alone (Me$_2$SO) or in the presence of actinomycin D (0.5 and 5.0 μM), and whole cell lysates were analyzed by immunoblot analysis for Sp1, ERα, and cyclin D1 proteins as described in Materials and Methods. Similar results showing that actinomycin D did not block proteasome-dependent degradation of cyclin D1 and ERα were also observed using DIM-C-pPhCF3 (15 μM; data not shown). **F,** effects of T007. MCF-7 cells were treated with different concentrations of T007 alone or in combination with DIM-C-pPhCF3 (15 μM) or PGJ2 (15 μM) for 20 h, and whole cell lysates were analyzed for cyclin D1, ERα, and Sp1 by Western blot analysis as described in Materials and Methods.

Although z-VAD-fmk partially blocks DIM-C-pPhC$_6$H$_5$-induced apoptosis (Fig. 6D), results suggest that caspase-independent pathways may be important, and these are currently being investigated.

PPARγ agonist-induced down-regulation of cyclin D1 is associated with inhibition of G$_0$/G$_1$-S phase progression in MCF-7 and other cell lines (25, 35, 60–62, 83). Results shown in Fig. 7 demonstrate that, like PGJ2, DIM-C-pPhCF$_3$ also decreased cyclin D1 and ERα proteins in MCF-7 cells within 1–3 h after treatment. Moreover, down-regulation of both proteins was reversed by proteasome (MG132) but not by protease (CII) inhibitors. Similar results were obtained for other C-substituted DIMs (data not shown) and ciglitazone (35) in MCF-7 cells. Actinomycin D did not block DIM-C-pPhC$_6$H$_5$- or PGJ2-induced down-regulation of cyclin D1 or ERα proteins, suggesting that these responses were associated with post-transcriptional pathways. The PPARγ inhibitor T007 also did not affect down-regulation

of cyclin D1 or ERα by PGJ2 or DIM-C-pPhCF$_3$ (Fig. 7F), indicating that this response was PPARγ independent as reported previously for PGJ2 in MCF-7 cells (60–62). Current studies are investigating the PPARγ-independent mechanisms of cyclin D1 and ERα degradation by C-substituted DIMs, other synthetic PPARγ agonists, and PGJ2.

In summary, this study shows that C-substituted DIMs are a novel class of PPARγ agonists that induce PPARγ-dependent transactivation and PPARγ-coactivator interactions in MCF-7 cells. C-substituted DIMs also induce responses observed for PGJ2 and other PPARγ agonists, and these include apoptosis, inhibition of cancer cell growth, inhibition of G_0/G_1-S phase progression, and enhanced Oil Red O staining in 3T3-L1 preadipocytes. Both PGJ2 and C-substituted DIMs induce proteasome-dependent down-regulation of cyclin D1 and ERα in MCF-7 cells. This response was PPARγ independent and consistent with results of previous studies with PGJ2 in MCF-7 cells (60–62). Currently, we are adapting other RNA interference methods (84, 85) for high efficiency and stable suppression of PPARγ in breast and other cancer cell lines to further investigate PPARγ-dependent and -independent pathways induced by C-substituted DIMs, PGJ2, and thiazolidinediones.

References

1. Rosen ED, Spiegelman BM. PPARγ: a nuclear regulator of metabolism, differentiation, and cell growth. J Biol Chem, 2001;276:37731–4.
2. Spiegelman BM, Flier JS. Adipogenesis and obesity: rounding out the big picture. Cell, 1996;87:377–89.
3. Kliewer SA, Willson TM. The nuclear receptor PPARγ—bigger than fat. Curr Opin Genet Dev, 1998;8:576–81.
4. Murphy GJ, Holder JC. PPAR-γ agonists: therapeutic role in diabetes, inflammation and cancer. Trends Pharmacol Sci, 2000;21:469–74.
5. Desvergne B, Wahli W. Peroxisome proliferator-activated receptors: nuclear control of metabolism. Endocr Rev, 1999;20:649–88.
6. Kersten S, Desvergne B, Wahli W. Roles of PPARs in health and disease. Nature, 2000;405:421–4.
7. Willson RM, Lambert MH, Kliewer SA. Peroxisome proliferator-activated receptor γ and metabolic disease. Annu Rev Biochem, 2001; 70:341–67.
8. Gupta RA, Brockman JA, Sarraf P, Willson TM, DuBois RN. Target genes of peroxisome proliferator-activated receptor γ in colorectal cancer cells. J Biol Chem, 2001;276:29681–7.
9. Itami A, Watanabe G, Shimada Y, et al. Ligands for peroxisome proliferator-activated receptor γ inhibit growth of pancreatic cancers both *in vitro* and *in vivo*. Int J Cancer, 2001;94:370–6.
10. Motomura W, Okumura T, Takahashi N, Obara T, Kohgo Y. Activation of peroxisome proliferator-activated receptor γ by troglitazone inhibits cell growth through the increase of $p27^{KiP1}$ in human. Pancreatic carcinoma cells. Cancer Res, 2000;60:5558–64.
11. Wächtershäuser A, Loitsch SM, Stein J. PPAR-γ is selectively upregulated in Caco-2 cells by butyrate. Biochem Biophys Res Commun, 2000;272:380–5.
12. Sato H, Ishihara S, Kawashima K, et al. Expression of peroxisome proliferator-activated receptor (PPAR)γ in gastric cancer and inhibitory effects of PPARγ agonists. Br J Cancer, 2000;83:1394–400.
13. Takahashi N, Okumura T, Motomura W, Fujimoto Y, Kawabata I, Kohgo Y. Activation of PPARγ inhibits cell growth and induces apoptosis in human gastric cancer cells. FEBS Lett, 1999;455:135–9.
14. Inoue K, Kawahito Y, Tsubouchi Y, et al. Expression of peroxisome proliferator-activated receptor γ in renal cell carcinoma and growth inhibition by its agonists. Biochem Biophys Res Commun, 2001;287: 727–32.
15. Kitamura S, Miyazaki Y, Hiraoka S, et al. PPARγ agonists inhibit cell growth and suppress the expression of cyclin D1 and EGF-like growth factors in *ras*-transformed rat intestinal epithelial cells. Int J Cancer, 2001;94:335–42.
16. Kubota T, Koshizuka K, Williamson EA, et al. Ligand for peroxisome proliferator-activated receptor γ (troglitazone) has potent antitumor effect against human prostate cancer both *in vitro* and *in vivo*. Cancer Res, 1998;58:3344–52.
17. Elnemr A, Ohta T, Iwata K, et al. PPARγ ligand (thiazolidinedione) induces growth arrest and differentiation markers of human pancreatic cancer cells. Int J Oncol, 2000;17:1157–64.
18. Kitamura S, Miyazaki Y, Shinomura Y, Kondo S, Kanayama S, Matsuzawa Y. Peroxisome proliferator-activated receptor γ induces growth arrest and differentiation markers of human colon cancer cells. Jpn J Cancer Res, 1999;90:75–80.
19. Elstner E, Muller C, Koshizuka K, et al. Ligands for peroxisome proliferator-activated receptor γ and retinoic acid receptor inhibit growth and induce apoptosis of human breast cancer cells *in vitro* and in BNX mice. Proc Natl Acad Sci USA, 1998;95:8806–11.
20. Chang TH, Szabo E. Induction of differentiation and apoptosis by ligands of peroxisome proliferator-activated receptor γ in non-small cell lung cancer. Cancer Res, 2000;60:1129–38.
21. Demetri GD, Fletcher CD, Mueller E, et al. Induction of solid tumor differentiation by the peroxisome proliferator-activated receptor-γ ligand troglitazone in patients with liposarcoma. Proc Natl Acad Sci USA, 1999; 96:3951–6.
22. Suh N, Wang Y, Williams CR, et al. A new ligand for the peroxisome proliferator-activated receptor-γ (PPAR-γ), GW7845, inhibits rat mammary carcinogenesis. Cancer Res, 1999;59:5671–3.
23. Sarraf P, Mueller E, Jones D, et al. Differentiation and reversal of malignant changes in colon cancer through PPARγ. Nat Med, 1998; 4:1046–52.
24. Clay CE, Namen AM, Atsumi G, et al. Influence of J series prostaglandins on apoptosis and tumorigenesis of breast cancer cells. Carcinogenesis, 1999;20:1905–11.
25. Wang CG, Fu MF, D'Amico M, et al. Inhibition of cellular proliferation through IκB kinase-independent and peroxisome proliferator-activated receptor γ-dependent repression of cyclin D1. Mol Cell Biol, 2001;21: 3057–70.
26. Patel L, Pass I, Coxon P, Downes CP, Smith SA, Macphee CH. Tumor suppressor and anti-inflammatory actions of PPARγ agonists are mediated via upregulation of PTEN. Curr Biol, 2001;11:764–8.
27. Pignatelli M, Cortes-Canteli M, Lai C, Santos A, Perez-Castillo A. The peroxisome proliferator-activated receptor γ is an inhibitor of ErbBs activity in human breast cancer cells. J Cell Sci, 2001;114:4117–26.
28. Ikezoe T, Miller CW, Kawano S, et al. Mutational analysis of the peroxisome proliferator-activated receptor γ gene in human malignancies. Cancer Res, 2001;61:5307–10.
29. Safe S. Modulation of gene expression and endocrine response pathways by 2,3,7,8-tetrachlorodibenzo-*p*-dioxin and related compounds. Pharmacol Ther, 1995;67:247–81.
30. Safe S, Wormke M, Samudio I. Mechanisms of inhibitory aryl hydrocarbon receptor-estrogen receptor crosstalk in human breast cancer cells. J Mammary Gland Biol Neoplasia, 2000;5:281–92.
31. Chen I, McDougal A, Wang F, Safe S. Aryl hydrocarbon receptor-mediated antiestrogenic and antitumorigenic activity of diindolylmethane. Carcinogenesis, 1998;19:1631–9.
32. McDougal A, Sethi-Gupta M, Ramamoorthy K, Sun G, Safe S. Inhibition of carcinogen-induced rat mammary tumor growth and other estrogen-dependent responses by symmetrical dihalo-substituted analogs of diindolylmethane. Cancer Lett, 2000;151:169–79.
33. McDougal A, Gupta MS, Morrow D, Ramamoorthy K, Lee Y-E, Safe S. Methyl-substituted diindolylmethanes as inhibitors of estrogen-induced growth of T47D cells and mammary tumors in rats. Breast Cancer Res Treat, 2001;66:147–57.
34. McDougal A. Aromatic hydrocarbon receptor-based antiestrogens as treatments for breast cancer [PhD dissertation]. Texas A&M University; 2000.
35. Qin C, Burghardt R, Smith R, Wormke M, Stewart J, Safe S. Peroxisome proliferator-activated receptor γ (PPARγ) agonists induce proteasome-dependent degradation of cyclin D1 and estrogen receptor α in MCF-7 breast cancer cells. Cancer Res, 2003;63:958–64.

36. Kamal A, Ali QA. Syntheses of some substituted di-indolyl-methanes in aqueous medium at room temperature. Tetrahedron, 1963;19:513 – 20.

37. Abdelrahim M, Samudio I, Smith R, Burghardt R, Safe S. Small inhibitory RNA duplexes for Sp1 mRNA block basal and estrogen-induced gene expression and cell cycle progression in MCF-7 breast cancer cells. J Biol Chem, 2002;277:28815 – 22.

38. Wormke M, Stoner M, Saville B, et al. The aryl hydrocarbon receptor mediates degradation of the estrogen receptor α through activation of proteasomes. Mol Cell Biol, 2003;23:1843 – 55.

39. Abdelrahim M, Smith 3rd R, Safe S. Aryl hydrocarbon receptor gene silencing with small inhibitory RNA differentially modulates Ah-responsiveness in MCF-7 and HepG2 cancer cells. Mol Pharmacol, 2003; 63:1373 – 81.

40. Xu HE, Lambert MH, Montana VG, et al. Structural determinants of ligand binding selectivity between the peroxisome proliferator-activated receptors. Proc Natl Acad Sci USA, 2001;98:13919 – 24.

41. Lee G, Elwood F, McNally J, et al. T0070907, a selective ligand for peroxisome proliferator-activated receptor γ, functions as an antagonist of biochemical and cellular activities. J Biol Chem, 2002;277:19649 – 57.

42. Klinge CM. Estrogen receptor interactions with co-activators and corepressors. Steroids, 2000;65:227 – 51.

43. Hu X, Lazar MA. Transcriptional repression by nuclear hormone receptors. Trends Endocrinol Metab, 2000;11:6 – 10.

44. Leo C, Chen JD. The SRC family of nuclear receptor coactivators. Gene, 2000;245:1 – 11.

45. Näär AM, Lemon BD, Tjian R. Transcriptional coactivator complexes. Annu Rev Biochem, 2001;70:475 – 501.

46. Rosenfeld MG, Glass CK. Coregulator codes of transcriptional regulation by nuclear receptors. J Biol Chem, 2001;276:36865 – 8.

47. Puigserver P, Wu Z, Park CW, Graves R, Wright M, Spiegelman BM. A cold-inducible coactivator of nuclear receptors linked to adaptive thermogenesis. Cell, 1998;92:829 – 39.

48. Knutti D, Kralli A. PGC-1, a versatile coactivator. Trends Endocrinol Metab, 2001;12:360 – 5.

49. Puigserver P, Spiegelman BM. Peroxisome proliferator-activated receptor-γ coactivator 1α(PGC-1α): transcriptional coactivator and metabolic regulator. Endocr Rev, 2003;24:78 – 90.

50. Näär AM, Beaurang PA, Zhou S, Abraham S, Solomon W, Tjian, R. Composite co-activator ARC mediates chromatin-directed transcriptional activation. Nature, 1999;398:828 – 32.

51. Ito M, Yuan CX, Malik S, et al. Identity between TRAP and SMCC complexes indicates novel pathways for the function of nuclear receptors and diverse mammalian activators. Mol Cell, 1999;3:361 – 70.

52. Rachez C, Lemon BD, Suldan Z, et al. Ligand-dependent transcription activation by nuclear receptors requires the DRIP complex. Nature, 1999; 398:824 – 8.

53. Sun X, Zhang Y, Cho H, et al. NAT, a human complex containing Srb polypeptides that functions as a negative regulator of activated transcription. Mol Cell, 1998;2:213 – 22.

54. Kodera Y, Takeyama K, Murayama A, Suzawa M, Masuhiro Y, Kato S. Ligand type-specific interactions of peroxisome proliferator-activated receptor γ with transcriptional coactivators. J Biol Chem, 2000;275: 33201 – 4.

55. Schlegel J, Peters I, Orrenius S, et al. CPP32/apopain is a key interleukin 1 β converting enzyme-like protease involved in Fas-mediated apoptosis. J Biol Chem, 1996;271:1841 – 4.

56. Garcia-Calvo M, Peterson EP, Leiting B, Ruel R, Nicholson DW, Thornberry NA. Inhibition of human caspases by peptide-based and macromolecular inhibitors. J Biol Chem, 1998;273:32608 – 13.

57. Han Z, Hendrickson EA, Bremner TA, Wyche JH. A sequential two-step mechanism for the production of the mature p17:p12 form of caspase-3 *in vitro.* J Biol Chem, 1997;272:13432 – 6.

58. Wyllie AH. Glucocorticoid-induced thymocyte apoptosis is associated with endogenous endonuclease activation. Nature, 1980;284:555 – 6.

59. Qi XM, He H, Zhong H, Distelhorst CW. Baculovirus p35 and Z-VAD-fmk inhibit thapsigargin-induced apoptosis of breast cancer cells. Oncogene, 1997;15:1207 – 12.

60. Straus DS, Glass CK. Cyclopentenone prostaglandins: new insights on biological activities and cellular targets. Med Res Rev, 2001;21:185 – 210.

61. Campo PA, Das S, Hsiang CH, Bui T, Samuel CE, Straus DS. Translational regulation of cyclin D1 by 15-deoxy-Δ(12,14)-prostaglandin J2. Cell Growth & Differ, 2002;13:409 – 20.

62. Clay CE, Monjazeb A, Thorburn J, Chilton FH, High KP. 15-Deoxy-Δ(12,14)-prostaglandin J2-induced apoptosis does not require PPARγ in breast cancer cells. J Lipid Res, 2002;43:1818 – 28.

63. Kristal AR, Lampe JW. *Brassica* vegetables and prostate cancer risk: a review of the epidemiological evidence. Nutr Cancer, 2002;42:1 – 9.

64. Murillo G, Mehta RG. Cruciferous vegetables and cancer prevention. Nutr Cancer, 2001;41:17 – 28.

65. Terry P, Wolk A, Persson I, Magnusson C. *Brassica* vegetables and breast cancer risk. JAMA, 2001;285:2975 – 7.

66. Preobrazhenskaya MN, Bukhman VM, Korolev AM, Efimov SA. Ascorbigen and other indole-derived compounds from *Brassica* vegetables and their analogs as anticarcinogenic and immunomodulating agents. Pharmacol Ther, 1993;60:301 – 13.

67. Bjeldanes LF, Kim JY, Grose KR, Bartholomew JC, Bradfield CA. Aromatic hydrocarbon responsiveness-receptor agonists generated from indole-3-carbinol *in vitro* and *in vivo*—comparisons with 2,3,7,8-tetrachlorodibenzo-*p*-dioxin. Proc Natl Acad Sci USA, 1991;88:9543 – 7.

68. Liu H, Wormke M, Safe S, Bjeldanes LF. Indolo[3,2-*b*]carbazole: a dietary factor which exhibits both antiestrogenic and estrogenic activity. J Natl Cancer Inst, 1994;86:1758 – 65.

69. Riby JE, Feng C, Chang Y-C, Schaldach CM, Firestone GL, Bjeldanes LF. The major tricyclic trimeric product of indole-3-carbinol is a strong agonist of the estrogen receptor signaling pathway. Biochemistry, 2000; 39:910 – 8.

70. Mazzei M, Miele M, Nieddu E, Barbieri F, Bruzzo C, Alama A. Unsymmetrical methylene derivatives of indoles as antiproliferative agents. Eur J Med Chem, 2001;36:915 – 23.

71. Beckers T, Reissmann T, Schmidt M, et al. 2-Aroylindoles, a novel class of potent, orally active small molecule tubulin inhibitors. Cancer Res, 2002;62:3113 – 9.

72. Mahboobi S, Teller S, Pongratz H, et al. Bis(1*H*-2-indolyl)methanones as a novel class of inhibitors of the platelet-derived growth factor receptor kinase. J Med Chem, 2002;45:1002 – 18.

73. Dominguez B, Vega MJ, Sussman F, de L. Synthesis and characterization of a new RXR agonist based on the 6-*tert*-butyl-1,1-dimethylindanyl structure. Bioorg Med Chem Lett, 2002;12:2607 – 9.

74. Dinnell K, Chicchi GG, Dhar MJ, et al. 2-Aryl indole NK1 receptor antagonists: optimization of the 2-aryl ring and the indole nitrogen substituent. Bioorg Med Chem Lett, 2001;11:1237 – 40.

75. Henke BR, Adkison KK, Blanchard SG, et al. Synthesis and biological activity of a novel series of indole-derived PPARγ agonists. Bioorg Med Chem Lett, 1999;9:3329 – 34.

76. Anzick SL, Kononen J, Walker RL, et al. AIB1, a steroid receptor coactivator amplified in breast and ovarian cancer. Science, 1997;277: 965 – 8.

77. Reiter R, Wellstein A, Riegel AT. An isoform of the coactivator AIB1 that increases hormone and growth factor sensitivity is overexpressed in breast cancer. J Biol Chem, 2001;276:39736 – 41.

78. Lauritsen KJ, List HJ, Reiter R, Wellstein A, Riegel AT. A role for TGF-β in estrogen and retinoid mediated regulation of the nuclear receptor coactivator AIB1 in MCF-7 breast cancer cells. Oncogene, 2002;21: 7147 – 55.

79. Janicke RU, Sprengart ML, Wati MR, Porter AG. Caspase-3 is required for DNA fragmentation and morphological changes associated with apoptosis. J Biol Chem, 1998;273:9357 – 60.

80. Janicke RU, Ng PA, Sprengart ML, Porter AG. Caspase-3 is required for α-fodrin cleavage but dispensable for cleavage of other death substrates in apoptosis. J Biol Chem, 1998;273:15540 – 5.

81. Kottke TJ, Blajeski AL, Meng XW, et al. Lack of correlation between caspase activation and caspase activity assays in paclitaxel-treated MCF-7 breast cancer cells. J Biol Chem, 2002;277:804 – 15.

82. Perillo B, Sasso A, Abbondanza C, Palumbo G. 17β-Estradiol inhibits apoptosis in MCF-7 cells, inducing *bcl-2* expression via two estrogen-responsive elements present in the coding sequence. Mol Cell Biol, 2000; 20:2890 – 901.

83. Palakurthi SS, Aktas H, Grubissich LM, Mortensen RM, Halperin JA. Anticancer effects of thiazolidinediones are independent of peroxisome proliferator-activated receptor γ and mediated by inhibition of translation initiation. Cancer Res, 2001;61:6213 – 8.

84. Barton GM, Medzhitov R. Retroviral delivery of small interfering RNA into primary cells. Proc Natl Acad Sci USA, 2002;99:14943 – 5.

85. Paddison PJ, Caudy AA, Hannon GJ. Stable suppression of gene expression by RNAi in mammalian cells. Proc Natl Acad Sci USA, 2002; 99:1443 – 8.

Molecular Cancer Therapeutics

A new class of peroxisome proliferator-activated receptor γ (PPAR γ) agonists that inhibit growth of breast cancer cells: 1,1-Bis(3′-indolyl)-1-(*p*-substituted phenyl)methanes

Chunhua Qin, Derek Morrow, Jessica Stewart, et al.

Mol Cancer Ther 2004;3:247-260.